The Astrophysical Journal, 736:78 (11pp), 2011 August 1 doi:10.1088/0004-637X/736/2/78

BROADBAND TRANSMISSION SPECTROSCOPY OF THE SUPER-EARTH GJ 1214b SUGGESTS A LOW MEAN MOLECULAR WEIGHT ATMOSPHERE*

Bryce Croll[1], Loic Albert[2], Ray Jayawardhana[1], Eliza Miller-Ricci Kempton[3], Jonathan J. Fortney[3], Norman Murray[4,6], and Hilding Neilson[5]
[1] Department of Astronomy and Astrophysics, University of Toronto, 50 St. George Street, Toronto, ON M5S 3H4, Canada; croll@astro.utoronto.ca
[2] Département de Physique, Université de Montréal, C.P. 6128 Succ. Centre-Ville, Montréal, QC H3C 3J7, Canada
[3] Department of Astronomy and Astrophysics, University of California, Santa Cruz, CA 95064, USA
[4] Canadian Institute for Theoretical Astrophysics, 60 St. George Street, University of Toronto, Toronto, ON M5S 3H8, Canada
[5] Argelander-Institut für Astronomie, Auf dem Hügel 71, D-53121 Bonn, Germany
Received 2010 October 11; accepted 2011 March 30; published 2011 July 7

ABSTRACT

We use the Wide-field Infrared Camera (WIRCam) on the Canada–France–Hawaii Telescope to observe four transits of the super-Earth planet GJ 1214b in the near-infrared. For each transit, we observe GJ 1214 in two bands nearly simultaneously by rapidly switching the WIRCam filter wheel back and forth for the duration of the observations. By combining all our *J*-band ($\sim$1.25 μm) observations we find a transit depth, analogous to the planet-to-star radius ratio squared, in this band of $(R_{PJ}/R_*)^2 = (1.338 \pm 0.013)\%$—a value consistent with the optical transit depth reported by Charbonneau and collaborators. However, our best-fit combined K_s-band ($\sim$2.15 μm) transit depth is deeper: $(R_{PKs}/R_*)^2 = (1.438 \pm 0.019)\%$. Formally, our K_s-band transits are deeper than the *J*-band transits observed simultaneously by a factor of $(R_{PKs}/R_{PJ})^2 = 1.072 \pm 0.018$—a 4σ discrepancy. The most straightforward explanation for our deeper K_s-band transit depth is a spectral absorption feature from the limb of the atmosphere of the planet; for the spectral absorption feature to be this prominent, the atmosphere of GJ 1214b must have a large-scale height and a low mean molecular weight. That is, its atmosphere would have to be hydrogen/helium dominated and this planet would be better described as a mini-Neptune. However, recently published observations from 0.78 to 1.0 μm, by Bean and collaborators, show a lack of spectral features and transit depths consistent with those obtained by Charbonneau and collaborators. The most likely atmospheric composition for GJ 1214b that arises from combining all these observations is less clear; if the atmosphere of GJ 1214b is hydrogen/helium dominated, then it must have either a haze layer that is obscuring transit-depth differences at shorter wavelengths or significantly different spectral features from what current models predict. Our observations disfavor a water-world composition, but such a composition will remain a possibility for GJ 1214b until observations reconfirm our deeper K_s-band transit depth or detect features at other wavelengths.

Key words: infrared: planetary systems – stars: individual (GJ 1214) – techniques: photometric

Online-only material: color figures

1. INTRODUCTION

Astronomers have been waiting for some time for a planet remotely similar to our own Earth that could be readily investigated with current instruments. Such an object was recently announced with the seminal discovery of the super-Earth planet GJ 1214b (Charbonneau et al. 2009) with the MEarth telescope network (Nutzman & Charbonneau 2008; Irwin et al. 2009). Although not the first transiting super-Earth announced—CoRoT-7b arguably holds that honor (Leger et al. 2009; Queloz et al. 2009; Pont et al. 2011)—GJ 1214b is in many ways more interesting as it offers the opportunity for advantageous follow-up to constrain its planetary characteristics. With a mass of 6.55 $M_\oplus$ and a radius of 2.68 $R_\oplus$, GJ 1214b's density ($\rho \sim 1.87$ g cm^{-3}; Charbonneau et al. 2009) is less than that of the terrestrial planets of our solar system and therefore GJ 1214b may have a significant gaseous atmosphere. Also, as it transits a low-mass star, its equilibrium temperature ($T_{\rm eq} \sim 500$ K assuming a low Bond albedo) is much more hospitable than that of CoRoT-7b, and it has a much more favorable planet-to-star radius ratio; as a result, if there are significant spectral features in its atmosphere then they should be detectable with current instruments.

As there are no super-Earth analogs in our solar system, it is a pressing question whether the burgeoning class of planets with minimum masses below 10 $M_\oplus$ (e.g., Udry et al. 2007; Mayor et al. 2009a, 2009b) are predominantly scaled-down Neptunes, with large helium–hydrogen atmospheric envelopes, or scaled-up terrestrial planets with atmospheres predominately composed of heavier molecules. Fortunately, GJ 1214b is an ideal candidate to answer such questions; Miller-Ricci & Fortney (2010) showed that due to GJ 1214b's advantageous scale height and planet-to-star radius ratio it should have readily observable water and methane spectral features across the infrared spectrum if its atmosphere is composed primarily of hydrogen and helium. Conversely, if its atmosphere is composed predominantly of heavier molecules, then the resulting smaller scale height will mute the spectral features and current instruments will return transit depths consistent with the depths measured in the optical by Charbonneau et al. (2009).

Furthermore, recent theoretical work has shown that measurements to constrain the composition of the gaseous atmosphere of GJ 1214b will also constrain the planet's bulk composition. Rogers & Seager (2010) and later Nettelmann et al. (2011) showed that the observed mass and radius (Charbonneau et al.

* Based on observations obtained with WIRCam, a joint project of CFHT, Taiwan, Korea, Canada, France, at the Canada–France–Hawaii Telescope (CFHT) which is operated by the National Research Council (NRC) of Canada, the Institute National des Sciences de l'Univers of the Centre National de la Recherche Scientifique of France, and the University of Hawaii.
[6] Canada Research Chair in Astrophysics.

2009) can be equally well fit by either a significant rocky core/mantle and a hydrogen-rich atmosphere or a "water-world" with a small water-rich core and a significant steam atmosphere. Searches for spectral features will differentiate between these two scenarios; detections of prominent spectral features will argue for the former scenario of a rocky core to go along with the hydrogen/helium-rich gaseous planetary envelope.

Recently, Bean et al. (2010) have performed just such transit spectroscopy observations using the FORS2 instrument on the Very Large Telescope (VLT); Bean et al. (2010) obtained 11 spectrophotometric light curves from 0.78–1.0 μm that show consistent transit depths with one another. By comparing to the Miller-Ricci & Fortney (2010) atmospheric models they were able to show that the lack of observed spectral features suggest that GJ 1214b must either have a high mean molecular weight and is likely a water-world, or its atmosphere is hydrogen/helium dominated with hazes or clouds high in the atmosphere that obscure the expected spectral features shortward of $\sim$1 μm. An additional possibility could certainly be that GJ 1214b's atmosphere is simply more complicated than expected, and its atmosphere could still be hydrogen/helium dominated with different spectral features from what the Miller-Ricci & Fortney (2010) models suggest.

We have also performed broadband transmission spectroscopy observations searching for GJ 1214b's spectral features from $\sim$1–2.5 μm using the Wide-field Infrared Camera (WIRCam) on the Canada–France–Hawaii Telescope (CFHT). We have already successfully demonstrated the precision of WIRCam on the CFHT in the near-infrared through our detections of the secondary eclipses and thermal emission for TrES-2b and TrES-3b in the K_s band (Croll et al. 2010a, 2010b), and for WASP-12b in the J, H and K_s bands (Croll et al. 2011). Here we report observations of several transits of the super-Earth GJ 1214b in three bands with WIRCam on the CFHT; for each transit we observed near-simultaneously in two bands to allow for accurate comparisons of the transit depths between these two bands. We observed an increased transit depth in the K_s band as compared to the J-band depth, likely indicative of absorption near $\sim$2.15 μm. The only way to achieve an absorption feature this prominent is if GJ 1214b has a large-scale height, a low mean molecular weight, and thus its atmosphere is hydrogen/helium dominated. We discuss below the likely possibilities for the atmospheric makeup of GJ 1214b that result from a combination of the Bean et al. (2010), Charbonneau et al. (2009), and our own data. Our results disfavor a water-world composition, but such a composition is possible if our K_s-band point is simply an outlier; such a composition will remain a distinct possibility until further observations either confirm our increased K_s-band depth or detect spectral features at other wavelengths. The observations to date are most qualitatively consistent with a hydrogen/helium-dominated atmosphere that is either hazy or one with more complicated spectral features than our current models suggest, such as an atmosphere where non-equilibrium chemistry plays a significant role.

2. OBSERVATIONS AND DATA REDUCTION

We observed the transit of GJ 1214b on four occasions with WIRCam on the CFHT. For each transit, we observed GJ 1214 in two bands nearly simultaneously by rapidly switching the WIRCam filter wheel back and forth between the two filters. We observed GJ 1214 alternating between the J ($\sim$1.25 μm) and K_s ($\sim$2.15 μm) filters on the evenings of 2010 June 27, 2010 August 15, and 2010 September 22. On the evening of 2010 August 7, we observed GJ 1214 alternating between the J and CH_4On filters ($\sim$1.69 μm); these 2010 August 7 observations were of a partial transit only, as the airmass of GJ 1214 increased during transit and during egress reached an airmass of $\sim$2.3, close to the hard limit of the telescope, preventing further observations. For the 2010 June 27 transit the airmass was low for the duration of the observations, while for the 2010 August 15 and 2010 September 22 transits the airmass increased throughout the observations and exceeded an airmass of two by the end of the out-of-transit baseline. For these latter two observations, we noticed that the data quality significantly degraded as the airmass rose above 2.0; therefore, for the analysis that follows we exclude the data in the out-of-transit baseline with an airmass greater than 2 for the 2010 August 15 and 2010 September 22 observations.

We observed GJ 1214 in Staring Mode (Devost et al. 2010) where we used the full WIRCam array with its $21' \times 21'$ field of view and did not dither for the duration of our observations. The only exception to our normal staring mode practice was the aforementioned filter change. The exposure times and defocus amounts for our various observations were: 3.5 s and 2.0 mm for the K_s band, 4 s and 1.2 mm for the CH_4On filter, and 3.5 s and 1.8 mm for the J band, respectively. The filter change during our observations induced an additional overhead of 20 s to switch the filter wheel, as well as an additional 60 s to take two acquisition images to fine-tune the target position and reinitiate guiding. We observed in data cubes of 12 exposures to increase the observing efficiency. We took 12 exposures (one guide cube) in a single filter, before performing the filter change and observing an additional 12 exposures in the other filter. The resulting duty cycles were: 22% for our J- and K_s-band observations, and 19% for our CH_4On and J-band observations.

The data were reduced and aperture photometry was performed on our target star and numerous reference stars. We used apertures with radii of 17, 18, and 15 pixels for our K_s, J, and CH_4On photometry, respectively; the associated inner and outer radii for the sky annuli were 21 and 29 pixels for our K_s-band and CH_4On photometry, and 22 and 30 pixels for our J-band photometry. We preprocessed our data using the I'iwi pipeline,[7] designed specifically for WIRCam imaging. We performed differential photometry on the target star with between 13 and 25 reference stars for our photometry in our various bands; for further details on the method we refer the reader to Croll et al. (2010a, 2010b). As can be seen in Figure 1, the out-of-transit photometry after subtraction of the background trend (Section 3) bins down near the Gaussian noise expectation with increasing bin size in all cases. Our data are therefore not seriously affected by time-correlated red noise. We set our errors for our transits equal to the root mean square (rms) of the data outside of transit after the subtraction of a linear trend; for our J and CH_4On photometry on 2010 August 7 we scale-up the errors from the rms by a factor of $\frac{5}{4}$ as these data are of a partial transit only, and the egress of transit occurs at very high airmass, which we found to be correlated with degraded precision with our other data sets. The resulting light curves for the various observations are displayed in the top panel of Figure 2.

3. RESULTS

We fit each of our data sets with a Mandel & Agol (2002) transit model, with the depth of transit, $(R_p/R_*)^2$, and the

[7] http://www.cfht.hawaii.edu/instruments/Imaging/WIRCam/liwiVersion1Doc.html

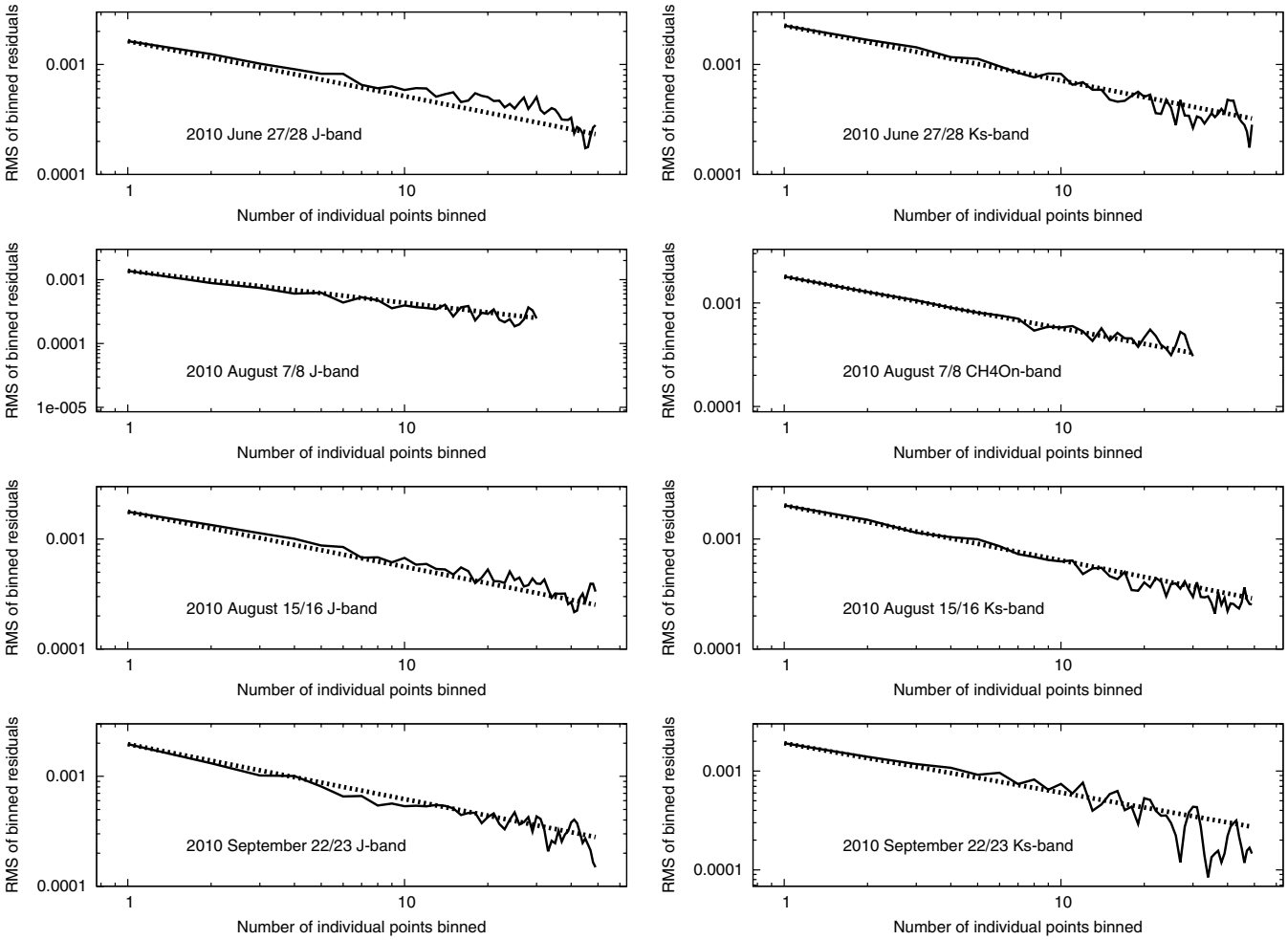

Figure 1. Root mean square of our out-of-eclipse photometry (solid line) after the subtraction of their respective background trends for our various data sets. The dashed line in each panel displays the one over the square root of the bin-size expectation for Gaussian noise.

best-fit mid-transit time as free parameters.[8] For several of our GJ 1214 data sets we noticed obvious trends with time after our differential photometry was performed, similar to the trends noticed in several of our existing WIRCam data sets (e.g., Croll et al. 2010a, 2010b, 2011). We cannot rule out that these trends are intrinsic to the target star and could be due to, for instance, long-term stellar variability as a result of rotational modulation. However, the frequency with which we observe such trends suggests that most of them are likely systematic in nature. We therefore refer to these trends as background trends, and we fit our data sets with linear or quadratic backgrounds of the form:

$$B_f = 1 + b_1 + b_2 dt + b_3 dt^2, \quad (1)$$

where dt is the time interval from the beginning of the observations and b_1, b_2, and b_3 are fit parameters. To determine whether a quadratic (b_3) term is justified to account for the background trend, we calculate the Bayesian information criterion (BIC; Liddle 2007), and ensure that the BIC is lower with the inclusion of the quadratic term. That is, the reduction in χ^2 must be sufficient to justify the extra degree of freedom. Only the August 15 K_s-band data warranted a quadratic term (b_3).

We employ Markov Chain Monte Carlo (MCMC) fitting as described in Croll (2006) and Croll et al. (2010a) using chains with 5×10^6 steps. There are four free parameters for each data set: $(R_p/R_*)^2$, the best-fit mid-transit time, b_1, and b_2. We also fit our data with the "residual-permutation" method (Winn et al. 2009) where the residuals to the best-fit data are shifted and refit, thus preserving the time correlation of any red noise in the data, so as to investigate the impact of time-correlated systematics. We find similar results to our MCMC analysis, although in general the errors are slightly larger. The increased size of the errors otherwise is likely due to low number statistics, as in this method for N data points one can only generate $2N$-1 light-curve permutations (~200–350 iterations for each of our data sets). For these reasons we quote our MCMC results henceforth.

We employ a quadratic limb-darkening law and obtain our limb-darkening parameters from Claret et al. (1998) for the J, K_s, and CH_4On filters; we adopt their H-band limb-darkening parameters for our CH_4On-filter observations. The Claret et al. (1998) limb-darkening parameters are calculated through fits to the PHOENIX stellar atmosphere models (Hauschildt et al. 1997a, 1997b). We employ the parameters c_2 and c_4 from nonlinear limb-darkening laws, as quoted in Table 1. For the input values that we use to generate the limb-darkening parameters we use approximations to the measured stellar effective temperature ($T_{\rm eff}$ = 3026 K), and log of the stellar surface gravity ($\log g = 4.991$ (CGS units), Charbonneau et al. 2009), of $T_{\rm eff}$ = 3000 K and $\log g$ = 5.0. We adopt the period and ephemeris of GJ 1214b given in Bean et al. (2010).

[8] We quote the barycentric Julian date in the terrestrial time standard using the routines of (Eastman et al. 2010).

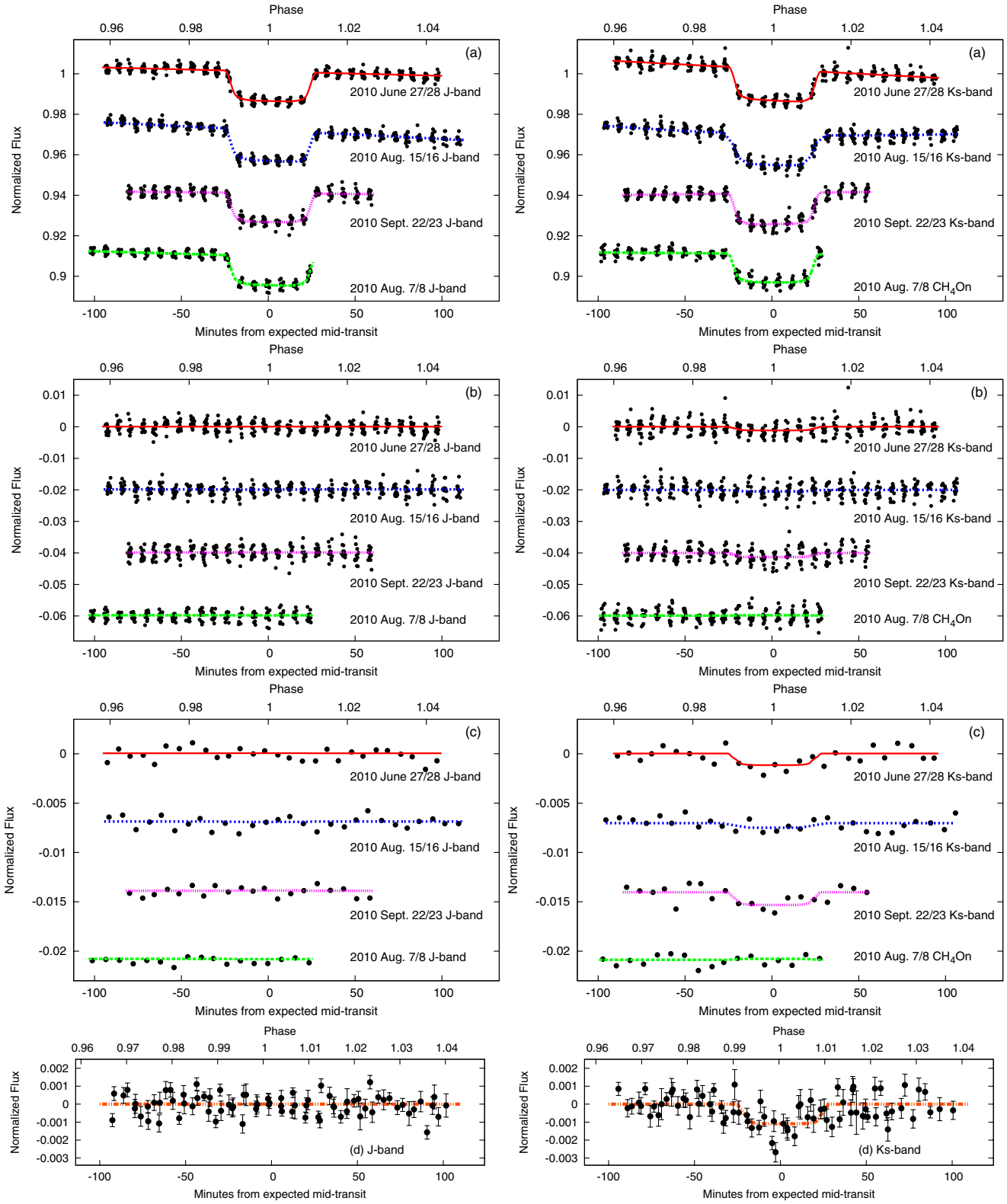

Figure 2. CFHT/WIRCam photometry bracketing the transit of GJ 1214 obtained nearly simultaneously on the nights denoted in the figure in the *J* band (left panels) and the K_s band and the CH_4On filter (right panels). The top set of panels (a) shows the data and the best-fit transit model displayed with the appropriately colored line. The second set of panels (b) shows the residuals of the data and the models from a transit model with a depth given by the best-fit value of the individual *J* band transits at left. Thus the (b) left panel simply displays the residuals from the best-fit transit model from that night's data. The (b) right panel displays the residuals of the K_s and CH_4On filter data and model from a transit with a depth equal to the best-fit *J*-band transit depth observed on that night nearly simultaneously and using the appropriate K_s or CH_4On limb-darkening coefficients. The third set of panels (c) is the same as the panels (b), except with the data binned every 12 points. The bottom panels (d) display all the data obtained simultaneously in the *J* and K_s bands from the panels (c) binned every 12 points (that is, the top three transit curves in the (a), (b), and (c) panels); the orange dot-dashed line displays the difference from the best-fit *J*-band transit model using the combined *J*- and K_s-band best-fit depths (Section 4). The errors in this panel are calculated from the standard deviation of the points within each bin. The best-fit K_s-band transits display increased transit depths, while the best-fit CH_4On transit displays a smaller transit depth than the *J*-band transits observed simultaneously. In the top three panels, the different data sets are offset vertically for clarity. Note that each set of panels has a different vertical scale.

(A color version of this figure is available in the online journal.)

Table 1
Characteristics of GJ 1214b's Atmosphere

Date in 2010	Filter	Fit Type[a]	Mid-transit Time (BJD-2450000)	$(R_p/R_*)^2$ (%)	$b1$	$b2$	$b3$	$c2$	$c4$
Jun 27	J	Ind.	$5375.8500^{+0.0001}_{-0.0002}$	$1.334^{+0.020}_{-0.021}$	$0.00542^{+0.00017}_{-0.00020}$	$-0.034^{+0.002}_{-0.002}$	n/a	1.24	−0.67
		Joint	$5375.8501^{+0.0001}_{-0.0001}$	$1.350^{+0.022}_{-0.018}$	$0.00543^{+0.00019}_{-0.00017}$	$-0.034^{+0.002}_{-0.002}$	n/a	$1.22^{+0.05}_{-0.04}$	$-0.69^{+0.04}_{-0.04}$
Jun 27	K_s	Ind.	$5375.8500^{+0.0002}_{-0.0001}$	$1.459^{+0.030}_{-0.029}$	$0.00780^{+0.00026}_{-0.00026}$	$-0.064^{+0.004}_{-0.003}$	n/a	1.06	−0.59
		Joint	$5375.8501^{+0.0001}_{-0.0001}$	$1.435^{+0.034}_{-0.034}$	$0.00777^{+0.00024}_{-0.00028}$	$-0.065^{+0.003}_{-0.003}$	n/a	$1.07^{+0.03}_{-0.05}$	$-0.57^{+0.04}_{-0.03}$
Aug 7	J	Ind.	$5416.9404^{+0.0001}_{-0.0001}$	$1.302^{+0.044}_{-0.040}$	$0.00624^{+0.00028}_{-0.00026}$	$-0.035^{+0.007}_{-0.008}$	n/a	1.24	−0.67
		Joint	n/a	n/a	n/a	n/a	n/a	n/a	n/a
Aug 7	CH_4On	Ind.	$5416.9402^{+0.0002}_{-0.0004}$	$1.290^{+0.050}_{-0.043}$	$0.00512^{+0.00035}_{-0.00031}$	$-0.010^{+0.008}_{-0.009}$	n/a	1.22	−0.66
		Joint	n/a	n/a	n/a	n/a	n/a	n/a	n/a
Aug 15	J	Ind.	$5424.8424^{+0.0004}_{-0.0002}$	$1.368^{+0.026}_{-0.021}$	$0.00739^{+0.00020}_{-0.00023}$	$-0.060^{+0.002}_{-0.003}$	n/a	1.24	−0.67
		Joint	$5424.8423^{+0.0001}_{-0.0001}$	$1.364^{+0.021}_{-0.024}$	$0.00734^{+0.00020}_{-0.00021}$	$-0.060^{+0.002}_{-0.002}$	n/a	$1.22^{+0.05}_{-0.04}$	$-0.69^{+0.04}_{-0.04}$
Aug 15	K_s	Ind.	$5424.8423^{+0.0001}_{-0.0001}$	$1.422^{+0.032}_{-0.034}$	$0.00703^{+0.00026}_{-0.00026}$	$-0.098^{+0.007}_{-0.002}$	$0.442^{+0.029}_{-0.056}$	1.06	−0.59
		Joint	$5424.8423^{+0.0001}_{-0.0001}$	$1.450^{+0.036}_{-0.036}$	$0.00708^{+0.00024}_{-0.00029}$	$-0.097^{+0.010}_{-0.003}$	$0.426^{+0.037}_{-0.066}$	$1.07^{+0.03}_{-0.05}$	$-0.57^{+0.04}_{-0.03}$
Sep 22	J	Ind.	$5462.7722^{+0.0002}_{-0.0002}$	$1.307^{+0.034}_{-0.031}$	$0.00493^{+0.00030}_{-0.00031}$	$-0.013^{+0.005}_{-0.005}$	n/a	1.24	−0.67
		Joint	$5462.7722^{+0.0001}_{-0.0001}$	$1.329^{+0.026}_{-0.028}$	$0.00497^{+0.00027}_{-0.00031}$	$-0.012^{+0.005}_{-0.006}$	n/a	$1.22^{+0.05}_{-0.04}$	$-0.69^{+0.04}_{-0.04}$
Sep 22	K_s	Ind.	$5462.7722^{+0.0002}_{-0.0002}$	$1.424^{+0.044}_{-0.031}$	$0.00406^{+0.00032}_{-0.00035}$	$0.016^{+0.006}_{-0.007}$	n/a	1.06	−0.59
		Joint	$5462.7722^{+0.0001}_{-0.0001}$	$1.412^{+0.039}_{-0.039}$	$0.00406^{+0.00028}_{-0.00038}$	$0.015^{+0.006}_{-0.006}$	n/a	$1.07^{+0.03}_{-0.05}$	$-0.57^{+0.04}_{-0.03}$

Note. [a] Fit Type stands for the joint or individual (Ind.) analyses.

We use the inclination and semimajor axis to stellar radius ratio[9] determined from an analysis from the Bean et al. (2010) white light curves (J. Bean 2010, private communication). All other parameters were fixed at the Charbonneau et al. (2009) values. Our best-fit MCMC transit and background fits for each of our individual transit data sets are listed in the "Ind." rows of Table 1 and displayed in the appropriately colored lines of Figure 2.

As discussed below (Section 4) we note a small, but significant, difference in the transit depths we measure in the J and K_s bands. To confirm that this difference is significant, and not due to any uncertainty in the limb-darkening coefficients,[10] we also fit our three J- and K_s-band transits simultaneously while fitting the two quadratic limb-darkening coefficients for each band (c_{2J}, c_{4J}, c_{2Ks}, and c_{4Ks}). We place a priori constraints on the limb-darkening coefficients; these priors on the limb-darkening coefficients are Gaussian with a standard deviation of 0.05 from the values derived from Claret et al. (1998) (and listed in the "Ind." rows of Table 1 for the J and K_s bands). For each of our three transits we fit the K_s- and J-band data sets with their own background terms (e.g., b_{1J}, b_{2J}, b_{1Ks}, and b_{2Ks} for the 2010 June 27 transit). We fit for the three mid-transit times of our three transits (to allow for possible transiting timing variations), but ensure that this value is held in common between the J- and K_s-band transits observed simultaneously. We fit for the J-band transit depths, but fit the K_s-band transits with a depth that is a consistent factor $(R_{PKs}/R_{PJ})^2$ greater than, or less than, the J-band transit observed nearly simultaneously for all three transits. By utilizing this fitting method, in addition to the methods discussed below in Section 4.3, we can directly ascertain how much deeper the K_s-band transits are than the J-band transits. The advantage of fitting for the depth of each of the J-band transits individually, rather than fitting them with a consistent depth, is that this allows for small variations in the J-band depth that could arise from rotational modulation (as discussed in Section 4.2), while still directly fitting for the ratio of the K_s- to J-band transit depths. We fit for 24 parameters overall, and the best-fit results are listed in the rows marked "Joint" analysis in Table 1.

3.1. WIRCam Nonlinearity Correction

We also ensured that any difference in the transit depth from the J to K_s bands was not due to an ineffective nonlinearity correction. During the I'iwi preprocessing step, a nonlinearity correction is applied to correct the count levels for pixels that approach saturation. Near saturation this nonlinearity correction can be as large as 10%. At the maximum count levels recorded in a pixel of the aperture of our target star, GJ 1214, during our observations, the detector is well below its saturation level, and the WIRCam detector is approximately 3%–5% nonlinear at these count levels. The vast majority of the pixels in our target star and reference star apertures are illuminated to much lower levels and are expected to be nonlinear at the 1%–3% level. If this nonlinearity correction was applied ineffectively then this could cause a systematic offset in our measured transit depths; although this discrepancy was expected to be much smaller than the difference in the transit depth from J to K_s that we measure, we nonetheless demonstrated this was the case by reprocessing and reanalyzing our 2010 September 22 transit data in the J and K_s bands without applying the nonlinearity correction. Any deviations in the pixel count values from the current nonlinearity correction will be more than an order of magnitude smaller than the effect induced by not applying the nonlinearity correction whatsoever. Not employing the nonlinearity corrections, as expected, leads to shallower transit depths than when the nonlinearity correction is applied. However, the ratio of the transit depths from K_s to J is near identical whether the nonlinearity correction is, or is not, applied. Overall, as this test should create a variation much larger than one due to an ineffective nonlinearity correction,

[9] An inclination of $i = 88.^{\circ}94$ and a semimajor axis to stellar radius ratio of $a/R_s = 14.97$.
[10] We also used quadratic limb darkening coefficients from Lester & Neilson (2008) and a model without limb-darkening. In both cases our K_s-band transit depths were significantly deeper than the J-band depths.

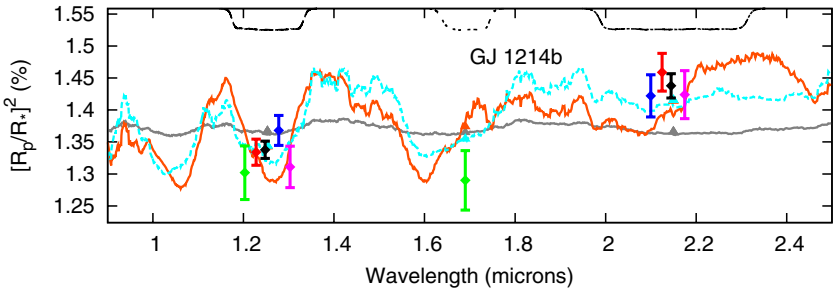

Figure 3. WIRCam transit observations of the super-Earth GJ 1214b. The WIRCam response functions are displayed inverted at the top of the plot using the black dotted lines at an arbitrary scale; these are from left to right: J band ($\sim$1.25 μm), the CH_4On filter ($\sim$1.69 μm), and K_s band ($\sim$2.15 μm). Our J- and K_s-band observations are indicated by the red diamonds for our 2010 June 27 observations, the blue diamonds for our 2010 August 15 observations, and the magenta diamonds for our 2010 September 22 observations. Our 2010 August 7 J-band and CH_4On-filter observations are indicated by the green diamonds. We offset our measured J and K_s observations slightly in wavelength for clarity. For the K_s and J bands we display the weighted mean and error of the observations in these bands with the black diamonds. The orange solid and cyan dashed curves are the Miller-Ricci & Fortney (2010) GJ 1214b atmospheric models for solar metallicity hydrogen/helium-dominated atmospheres (with and without methane, respectively). The gray dotted curve is the Miller-Ricci & Fortney (2010) models for an H_2O/steam atmosphere. We integrate the Miller-Ricci & Fortney (2010) atmospheric models over the WIRCam response functions and display these values in the appropriately colored solid triangles.

(A color version of this figure is available in the online journal.)

it is safe to conclude that the greater K_s-band than J-band transit depth does not arise from the nonlinearity correction.

4. DISCUSSION

4.1. GJ 1214b's Transit Depth in the Near-infrared

We display our best-fit transit depths in Figure 3 and Table 1. The J-band transit depths are largely consistent with one another and also with, or at most insignificantly shallower than, the depths reported by (Charbonneau et al. 2009) and Bean et al. (2010) in the optical and very near-infrared. The K_s-band transits also display similar depths to one another. However, the K_s-band transits appear to be deeper than the J-band transits; this is a small effect, but is clearly visible in the bottom panel of Figure 2 where we present the residuals of our observations from the best-fit J-band transit depths observed nearly simultaneously.

The CH_4On transit depth, on the other hand, appears to have a similar transit depth to the J-band transit observed simultaneously on 2011 August 7. As this is a partial transit only, and as much of the transit and the egress of transit occurs at very high airmass, caution is warranted in any robust comparison of the J to CH_4On transit depth and to other wavelengths.

By combining all the K_s-band and J-band transits, we find the weighted means and the associated errors on the transit depths are $(R_{pJ}/R_*)^2 = 1.338 \pm 0.013\%$ for the J band, and $(R_{pKs}/R_*)^2 = 1.438 \pm 0.019\%$ for the K_s band. As we only have one partial transit of GJ 1214 in the CH_4On filter, the depth in that band is simply the value from the 2010 August 7 transit: $(R_{p\mathrm{CH_4On}}/R_*)^2 = 1.290^{+0.050}_{-0.043}\%$. We determine the error on the weighted mean of our J-band and K_s-band points by determining the weighted error of all our observations in that particular band and then scaling that error upward by a factor of ζ. To determine ζ we calculate the χ^2 of all our data in a single band compared to a model with a consistent transit depth equal to the weighted mean of the transit depths in that band; we then scale-up the errors to ensure the reduced χ^2 is equal to one.[11] The K_s-band data points are consistent with one another, so only the J-band errors are scaled upward. The resulting value is $\zeta_J = 1.02$ for the J-band photometry, so this suggests that both the K_s- and J-band weighted errors are already appropriately sized, or close to it. Overall, this analysis suggests that our K_s-band and J-band transit depths are inconsistent with one another; the K_s-band transit depth is deeper than the J-band depth with 5σ confidence.

4.2. The Effect of Stellar Spots on Transit Observations of GJ 1214b

Charbonneau et al. (2009) reported that GJ 1214 is an active star and displays longer-term variability with a period of several weeks at the 2% level in the MEarth bandpass. More recently, Berta et al. (2010) presented and analyzed MEarth photometry of GJ 1214 from 2008 to 2010 and observed long-term photometric variability at the 1% level with a period of approximately 50 days. This variability is presumably due to rotational modulation from spots rotating in and out of view. As the long-term photometric monitoring presented in Berta et al. (2010) ends in 2010 July (in the midst of the observations we present here), we assume the more conservative limit of 2% variability for our calculations henceforth.

Transit observations obtained at different epochs may show small differences in the transit depth due to rotational modulation arising from both occulted and unocculted spots (Czesla et al. 2009; Berta et al. 2010; Carter et al. 2011). In the case of unocculted spots, if the 2% observed rotational modulation represents the full range from a spotted to unspotted photosphere[12] then we may expect measurements of the transit depth of GJ 1214b will vary by as much as 0.03% of the stellar signal in the MEarth bandpass (assuming an unspotted transit depth of 1.35%) from observations taken at epochs spanning the maximum and the minimum of the observed rotational modulation. On the other hand, occulted spots will cause small brightening events during the transit that may lead one to underestimate the true transit depth. Thus, for transit-depth measurements obtained at different epochs, such as our own, it is possible that the

[11] Andrae et al. (2010) note that there are several hidden assumptions one should be careful to address when applying reduced χ^2 to one's data; we feel the method we apply here should be useful nonetheless as a first-order approximation to indicate the appropriate size of the weighted error bars.

[12] There is no reason to expect we ever observe a hemisphere of the star free of spots altogether, and indeed the analysis of Carter et al. (2011) and Berta et al. (2010) suggests we very well may not, which would lead to larger transit-depth differences from epoch to epoch. Exact analytical expressions are available in Carter et al. (2011).

variability caused by rotational modulation creates small differences in the measured depths for observations taken at different epochs.

However, for our data obtained nearly simultaneously in two different bands, the effect of spots should be reduced for the following reasons. First of all, as the stellar rotation period of GJ 1214 appears to be much longer (Charbonneau et al. 2009; Berta et al. 2010) than the ∼1 hr duration of the transit, the spot pattern should be essentially static during a single transit. Secondly, even if the star is very spotted during our own observations, the difference between the transit depths measured nearly simultaneously in our two bands will be minute. This small difference will arise due to the differing ratio of the Planck function of the spot and the star due to their different temperatures; however, this difference will be muted as we move into the near-infrared. For instance, assuming that GJ 1214 has spots 500 K cooler—a value supposedly consistent with another M4.5 dwarf (Zboril et al. 2003)—than GJ 1214's ∼3000 K effective temperature (Charbonneau et al. 2009), the 2.0% variability due to rotational modulation in the MEarth bandpass (∼780 nm), will translate into 1.5%, and 1.0% variability in the J band and K_s band, respectively. Assuming the unspotted transit depth is 1.350% in these bands then the maximum transit depths from unocculted spots, which would result from measurements at the minimum flux of the observed rotational modulation, would be 1.369% in the J and 1.364% in the K_s band. The variation in the transit depth between the J and K_s bands that we observe is both much larger than this predicted effect due to starspots, and also would serve to create a deeper transit in J band rather than K_s band; we, of course, observe the opposite phenomenon.

A deeper K_s-band than J-band transit could arise from spots along the transit chord that are occulted during the observations. Occultation of spots by a planet will create anomalous brightenings during transit, as has been observed for the transiting planets HD 189733b (Pont et al. 2007), TrES-1b (Rabus et al. 2009; Dittmann et al. 2010), and more recently for GJ 1214b (Bean et al. 2010; Berta et al. 2010; Carter et al. 2011). However, due to the near-simultaneous nature of our photometry, it is unlikely that occulting spots could account for the variation in K_s- to J-band transit depth that we observe, again due to the small difference in the Planck functions of the spot relative to the star between our two bands. For instance, occulting a spot 500 K cooler than the surrounding photosphere that is 30% of the planetary size will lead to transits that are 0.07% shallower for the duration of the occultation than the presumed 1.35% transit depth in the J band. However the K_s-band transit depth will also be 0.05% shallower; the 0.02% relative difference between the two bands expected from a spot occultation is much less than the observed transit-depth difference we observe. Lastly, as spot occultations will lead to overall shallower transit depths, one would require the true transit depth of GJ 1214b to be deeper than that observed in our own J-band observations and in the optical and very near-infrared (Charbonneau et al. 2009; Bean et al. 2010). For these reasons we find it unlikely that the transit-depth difference we observe arises from occulted or unocculted spots.

4.3. A Larger Transit Depth in the K_s Band than the J Band

Due to the aforementioned possible variations in the transit depths from epoch to epoch induced by spots, a more straightforward method to compare the depths of transits in our bands is to directly compare the depth of the transit in one band to the depth obtained simultaneously in another—that is $(R_{PKs}/R_{PJ})^2$ for each one of our transits observed simultaneously in the K_s and J bands. We ignore our data observed on 2010 August 7 for this analysis, as GJ 1214 was observed in the J band and the CH_4On filter rather than in J and K_s.

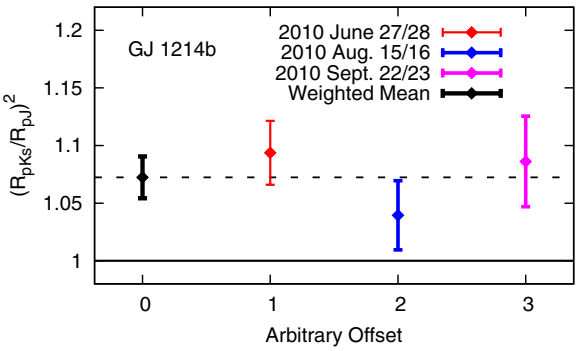

Figure 4. Measured K_s-band transit depth divided by the measured J-band transit depth for the "Ind." analysis of our various observations (see the legend). The horizontal dotted line denotes the weighted mean of the K_s- divided by J-band transit depth, $(R_{PKs}/R_{PJ})^2$. The solid horizontal solid line denotes the value if the K_s-band transits were the same depth as the J-band transits.

(A color version of this figure is available in the online journal.)

We attempt to measure the fraction that the K_s-band transits are deeper than the J-band transits, $(R_{PKs}/R_{PJ})^2$, by two methods. In the first method, we display the best-fit MCMC transit depth of our K_s-band photometry divided by the J-band transit depth from our individual analysis ("Ind.") in Figure 4. The associated errors displayed in this figure are generated by propagating through the associated errors on the individual best-fit MCMC transit depths as displayed in Table 1. The weighted mean and error of these data indicates that the K_s-band transits are deeper than the J-band transits by a factor of $(R_{PKs}/R_{PJ})^2 = 1.072 \pm 0.018$. The associated errors do not need to be scaled up, as the reduced χ^2 is near one for a comparison of our three $(R_{PKs}/R_{PJ})^2$ data points as compared to the weighted mean of these observations; specifically $\chi^2 = 1.92$, which is reasonable given the two degrees of freedom.[13] By analyzing the individual transits, our K_s-band photometry displays a deeper transit depth than our J-band photometry observed nearly simultaneously with a confidence in excess of 4σ.

In the second method we use the "Joint" MCMC analysis described above where we simultaneously fit the three data sets that observe in the K_s band and J band simultaneously. We fit each J-band transit with an independent transit depth, but assume that all the K_s-band transits were a consistent factor deeper (or shallower) than the J-band transits observed nearly simultaneously $(R_{PKs}/R_{PJ})^2$. We also fit the limb-darkening parameters after applying a Gaussian a priori assumption as described in Section 3. We display this ratio for our "Joint" analysis in Figure 5; we measured this fraction as $(R_{PKs}/R_{PJ})^2 = 1.063^{+0.019}_{-0.021}$. This distribution is not a perfect Gaussian, and therefore, according to this method our K_s-band transits are deeper than our J-band transits with greater than 3σ confidence.

Both methods return reasonably similar results, and argue for a deeper K_s-band transit depth than J-band transit depth with a confidence in excess of 3σ. We quote the value of $(R_{PKs}/R_{PJ})^2$ from our "Ind." results henceforth.

[13] We again note that there are several hidden assumptions one should be aware of when applying reduced χ^2 as documented in Section 4.1.

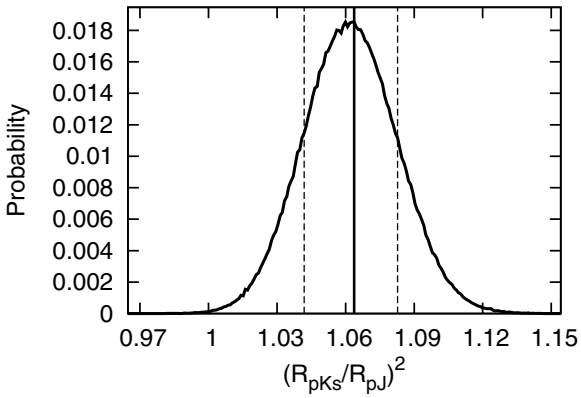

Figure 5. Measured K_s-band transit depth divided by the measured J-band transit depth from our "Joint" analysis. The vertical solid line denotes the best-fit value, while the dotted vertical lines indicate the 68% credible regions.

4.4. WIRCam Transit Depths Suggest a Low Mean Molecular Weight

The transit depths from our CFHT/WIRCam photometry suggests that GJ 1214b should have a large-scale height, low mean molecular weight and thus a hydrogen/helium-dominated atmosphere. These conclusions arise from the fact that our K_s-band transit depths are deeper than our J-band transit depths by a factor of $(R_{PKs}/R_{PJ})^2 = 1.072 \pm 0.018$. This corresponds to a relative change in the radius of GJ 1214b from the K_s band to the J band of 1.04%, or ~610 km compared to GJ 1214b's radius of ~17070 km. Using its equilibrium temperature of $T_{eq} \sim 560$ K (the value obtained assuming zero bond albedo) this amounts to absorption increasing the radius of GJ 1214b by ~2 atmospheric scale heights for a hydrogen gas envelope (H_2). As the molecular weight of H_2O is approximately nine times greater than hydrogen gas, a spectral feature this prominent assuming a water-world composition would require an increase in the planetary radius of ~20 atmospheric scale heights. This suggests that an atmosphere dominated by light elements is much more probable than one composed of heavier elements.

The change in transit depth due to a change in planetary radius between the line, R_{PL}, and the continuum, R_{PC}, can be related to the scale height, H, and the opacities in the absorption line, κ_l, and the continuum, κ_c; this value can be approximated by the ratio of the opacities multiplied by the area of an annulus one scale height thick relative to that of the stellar disk:

$$(R_{PL}/R_*)^2 - (R_{PC}/R_*)^2 = \frac{2\pi R_P H}{\pi R_*^2} \ln(\kappa_l/\kappa_c) \qquad (2)$$

(Brown et al. 2001). To cause the observed transit-depth difference in a hydrogen gas atmosphere would require line opacity marginally greater than that of the continuum ($\kappa_l/\kappa_c \sim 8$); the water-world composition would require an opacity that is unrealistically larger than that of the continuum ($\kappa_l/\kappa_c \sim 2 \times 10^8$). Therefore from our CFHT/WIRCam observations, one would expect that the atmosphere of GJ 1214b must have a low mean molecular weight, a large-scale height, and thus an atmosphere dominated by hydrogen and/or helium.

We compare our data to the Miller-Ricci & Fortney (2010) atmospheric models of GJ 1214b in Figure 3. We first employ the most conservative scenario and assume that due to rotational modulation, or other systematic errors, that we cannot directly compare our measured transit depths to the Charbonneau et al. (2009) or Bean et al. (2010) depths. We thus scale-up or scale-down the predicted absorption of the Miller-Ricci & Fortney (2010) models by a multiplicative factor, analogous to an increase or decrease of the squared ratio of the planetary to stellar radius, to produce the best-fit (minimum χ^2) compared to our observations. We display the Miller-Ricci & Fortney (2010) water-world model (an H_2O-dominated world) in the dotted gray line. We compare to two hydrogen/helium-dominated atmospheres; the first has solar-metallicity (orange dot-dashed line) while the second has solar metallicity but does not feature methane (cyan dot-dashed line). We integrate these models over the WIRCam response functions and calculate the associated χ^2 of our data compared to the model. Although we cannot strongly differentiate between hydrogen–helium envelopes with solar metallicity ($\chi^2_{\rm solar} = 9$) from those without methane ($\chi^2_{\rm no\text{-}methane} = 7$), the water-world composition is disfavored ($\chi^2_{H_2O} = 26$) by greater than 2σ for our seven degrees of freedom. Other high mean molecular weight models (e.g., the Miller-Ricci & Fortney (2010) CO_2-dominated or H_2O/CO_2-mixture atmospheres) are disfavored with similar confidence. The support for the hydrogen/helium composition arises from the observed increased absorption in K_s-band as opposed to our J-band observations. The CH_4On filter is nominally 1σ discrepant from the observed models; it is unclear at this present time whether this discrepancy is physical or simply due to low signal-to-noise.

4.5. Comparison to Observations at Other Wavelengths

Arguably, completely excluding the constraints imposed by transit-depth observations at other wavelengths, because of the effects of spots or systematic effects, is unnecessarily conservative. Therefore, we also compare the weighted means of our transit-depth measurements and the Miller-Ricci & Fortney (2010) models to the Charbonneau et al. (2009) depth measurement in the MEarth bandpass, the J-band measurement of Sada et al. (2010), and the Bean et al. (2010) measurements from 0.78–1.0 μm in Figure 6. We do not attempt to make a correction for the possibly variable spot activity between the various epochs at which the data were obtained; as discussed above in Section 4.2 rotational modulation can be expected to induce spurious transit-depth variations as large as 0.03% of the ~1.35% transit depth of GJ 1214b near 1 μm and will cause smaller variations at longer wavelengths. Also, a small discrepancy will be induced by the fact that the Sada et al. (2010) and Charbonneau et al. (2009) transit-depth measurements were produced with the original Charbonneau et al. (2009) estimates of the inclination and other parameters for this system, rather than the values derived from the Bean et al. (2010) white light photometry that we use here and that have been applied to the Bean et al. (2010) spectrophotometry. For these reasons, we caution that this comparison should be considered illustrative rather than definitive.

Of the original Miller-Ricci & Fortney (2010) atmospheric models the heavy mean molecular weight models, such as the water-world composition model ($\chi^2_{H_2O} = 40$), are highly favored over the low mean molecular weight compositions ($\chi^2_{\rm solar} = 101$ for the solar metallicity hydrogen/helium-dominated envelope).[14] The water-world composition is favored over the solar metallicity hydrogen/helium-dominated model with more than 5σ confidence. This is unsurprising, as it is largely the conclusion of the Bean et al. (2010) paper, and results from the high precision of the VLT/FORS2 spectrophotometry and the lack of

[14] As explained above in Section 4.4, we scale the radii of the planet in the models up or down to achieve the minimum χ^2 compared to the data.

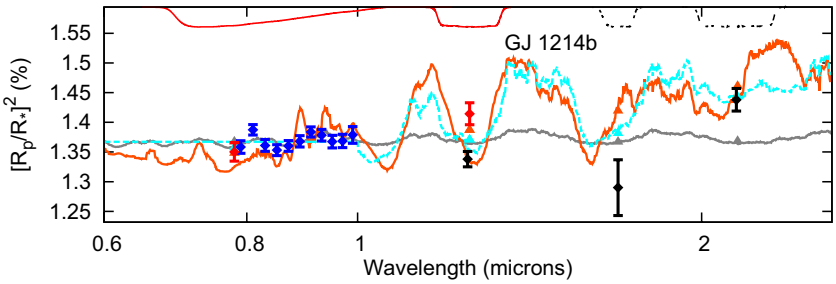

Figure 6. Transit observations of the super-Earth GJ 1214b. The response functions are displayed inverted at the top of the plot at arbitrary scale. These are from left to right the MEarth (∼0.78 μm), and Kitt-peak J band (∼1.25 μm) displayed in the red curves, and the WIRCam J band (∼1.25 μm), CH_4On filter (∼1.69 μm), and K_s band (∼2.15 μm) displayed in the black dotted curves. The Kitt-peak J-band bandpass overlaps the CFHT J-band bandpass. The VLT/FORS2 response functions are not included, as they essentially overlap with the points. The weighted mean of our J-band, K_s-band, and CH_4On-filter observations are displayed by the black diamonds. The MEarth (Charbonneau et al. 2009) and the Kitt-peak Sada et al. (2010) transit depth are displayed with the red diamonds, while the VLT/FORS2 points (Bean et al. 2010) are displayed with blue diamonds. We display two Miller-Ricci & Fortney (2010) GJ 1214b atmospheric models (a water-world model (gray dotted curve) and a solar-metallicity model (orange solid curve)); the other model we present in the cyan dashed curve is a Miller-Ricci & Fortney (2010) solar-metallicity no methane model at wavelengths longer than 1 μm, while at shorter wavelengths we arbitrarily cutoff the predicted absorption to simulate the impact of putative hazes. We integrate these atmospheric models over the WIRCam response functions and display these values in the appropriately colored solid triangles. We caution that this comparison does not correct the depths for possible variability due to rotational modulation and thus any comparison should be considered illustrative rather than definitive.

(A color version of this figure is available in the online journal.)

observed spectral features in the very near-infrared. The Bean et al. (2010) paper excludes the expected methane and water spectral absorption features from a hydrogen/helium-dominated atmosphere from 0.78 to 1.0 μm with high confidence.

Another possibility to explain the lack of observed spectral features are high-altitude hazes (Fortney 2005) in the atmosphere of GJ 1214b that could mute the spectral features at shorter wavelengths. We discuss this possibility further below (Section 4.6). We thus also compare our observations to a no-methane model where we cut off the absorption below 1 μm and set it equal to a nominal value of 1.35%. At wavelengths greater than 1 μm, the values are identical to the no-methane model. This abrupt transition is not intended to be physical, but simply illustrative of the impact hazes could have on the expected transmission spectrum at shorter wavelengths.[15] This model has the lowest χ^2 ($\chi^2_{\text{hazy-hydrogen}} = 34$) of any of the models as it is able to address the lack of observed spectral features in the Bean et al. (2010) spectrophotometry, and our deeper K_s-band depth compared to our J-band depth. We note that the improvement in the χ^2 of this haze model to the water-world model is not significant, and both remain leading candidates to explain all the observations of GJ 1214 to date, as discussed below.

4.6. Possible Atmospheric Compositions of GJ 1214b

All the transmission spectroscopy observations of GJ 1214b to date could be explained by a high mean molecular weight atmosphere if our deeper K_s-band transit is simply an outlier. If GJ 1214b's atmosphere does have a high mean molecular weight, a water-vapor atmosphere is a leading possibility. This water-world scenario will remain a viable candidate until observations are performed to confirm that either our K_s-band transit depths are indeed deeper or spectral features are detected at other wavelengths.

A scenario that would qualitatively explain all the observations to date, is a hydrogen/helium-dominated atmosphere with thick hazes that would mute the presence of spectral features arising from shorter wavelengths due to scattering. This haze layer would have to be at high altitudes, and low pressures (<200 mbar), to effectively mute the expected spectral features that would arise from being able to stare deep into the atmosphere of the planet in opacity windows in the very near-infrared. The efficiency of scattering diminishes for wavelengths longer than the approximate particle size (Hansen & Travis 1974). The haze particles could not be much smaller than sub-micron size to account for the lack of observed spectral features in the Bean et al. (2010) spectrophotometry in the very near-infrared. Due to the expected size of these putative haze particles, shorter wavelength optical observations would not be expected to show simply the monotonic increase in planetary radius expected from a Rayleigh scattering signal, but instead the more complicated transmission spectrum signal of Mie scattering (see, for example, Lecavelier des Etangs et al. 2008).

Such a haze or cloud layer is certainly not inconceivable. A cloud deck or haze has been reported to mute the optical transmission spectrum from 0.29 to 1.05 μm of the hot Jupiter HD 189733b (Pont et al. 2008; Sing et al. 2011); in the infrared HD 189733b may have absorption features with an opacity even greater than those that result from the haze at those wavelengths (Desert et al. 2011). The hazes of Jupiter and Titan may be other suitable analogies. Titan has a haze layer that is optically thick in the optical, but has transparent windows as one moves into the near-infrared (Tomasko et al. 2008; Griffith et al. 1993). The opacity of hazes on Jupiter are high at short optical wavelengths, but are much smaller as one moves into longer optical wavelengths and into the near-infrared (Rages et al. 1999).

A potential culprit for the particle causing this haze is a hydrocarbon derived from the photochemical destruction of methane (Moses et al. 2005; Zahnle et al. 2009). Methane is found in the atmospheres of all the solar system's giant planets, as well as that of Titan. The end products of the breakdown of methane are higher-order hydrocarbons that condense as solids (Rages et al. 1999). Since GJ1214b should be relatively cool ($T_{\text{eq}} \sim 500$ K) its atmospheric carbon inventory could feature abundant methane, like that of Jupiter. Particulates with a relatively small mixing ratio can have important effects at the slant viewing geometry appropriate for transits (Fortney 2005), and thus hydrocarbons in a high-altitude haze are one possible explanation the lack of observed features in the Bean et al. (2010) spectrophotometry.

[15] Depending on the size of the particles one would expect the observed transit radius to increase at very short wavelengths due to Rayleigh scattering or have a more complicated behavior due to Mie scattering.

We finally note that the actual spectral features of GJ 1214b, whether its atmosphere is hydrogen/helium dominated or not, could be more complicated and thus very different from what the Miller-Ricci & Fortney (2010) models predict. One such reason could be the impact of non-equilibrium chemistry (Miller-Ricci Kempton et al. 2011).

Clearly further observations are required to differentiate between these scenarios and determine the true atmospheric makeup of GJ 1214b.

4.6.1. An Opacity Source at ~2.15 μm

The increased transit depths we note in our K_s-band observations argue for an opacity source near ~2.15 μm that is causing increased absorption along the limb of the planet. One such possible opacity source is methane, which is predicted to cause absorption from ~2.2 to ~2.4 μm in the Miller-Ricci & Fortney (2010) hydrogen/helium-dominated atmospheric models. Although our K_s-band transit depth is qualitatively consistent with this methane spectral absorption feature, we note that the Miller-Ricci & Fortney (2010) hydrogen/helium model with solar metallicity, but without methane, provides a near-identical goodness-of-fit as compared to the solar metallicity model with methane. This is because the methane absorption feature is present at the red edge of our K_s band only; on the blue edge of the K_s band the hydrogen/helium model with methane actually features less absorption than the model without methane, so overall the predicted transit depth is similar whether methane is or is not present according to the Miller-Ricci & Fortney (2010) prediction. Also, greater concentrations of methane in the atmosphere are not expected to cause increased absorption at these wavelengths. In the no-methane model, the increased K_s-band absorption compared to J-band results from water opacity. Thus both water and methane remain viable candidates for this increased absorption. Both these molecules should also lead to spectral features from 0.78 to 1.0 μm that have been ruled out by the Bean et al. (2010) spectrophotometry at high confidence. Thus for these chemicals to remain viable opacity sources, one requires the presence of hazes in the atmosphere of GJ 1214b, or that the spectral features are more complicated than the Miller-Ricci & Fortney (2010) models predict. We encourage further modeling to elucidate whether this ~2.15 μm feature is due to methane, water or another opacity source.

4.7. Consequences of a Hydrogen/Helium-dominated Atmosphere

A hydrogen/helium-dominated atmosphere on GJ 1214b would be expected to undergo significant hydrodynamic escape. Therefore, if GJ 1214b is hydrogen/helium dominated then it may have lost, or is losing, a significant fraction of its gaseous envelope. Charbonneau et al. (2009) and Rogers & Seager (2010) predicted that if GJ 1214b's atmosphere is dominated by hydrogen gas then it will lose on the order of $\sim 10^9$ g s^{-1}, or ~0.02 $M_\oplus$ on a 4 Gyr timescale.[16] As its host star may have been more active earlier in its life, and thus brighter in the ultraviolet, its cumulative mass loss may be higher. Thus, either if GJ 1214b's hydrogen/helium envelope is primordial or due to outgassing we may expect it to have lost, and will be losing, a non-negligible fraction of its atmosphere.

Also, Carter et al. (2011) have pointed out that the radius of the star, GJ 1214, that one obtains from stellar evolutionary models is very different from the radius one obtains from an analysis of the light curve. As a result the density of GJ 1214b varies accordingly, from one where a significant gaseous atmosphere is likely, to a much higher density where one would only expect a thin gaseous atmosphere on top of a solid terrestrial planet. Our increased K_s-band transit depth argues in favor of the lighter density and the stellar radius suggested by fits to light-curve parameters.

[16] Charbonneau et al. (2009) report a 3–10 Gyr age for this system.

4.7.1. Constraints on GJ 1214b's Bulk Composition

If the atmosphere of GJ 1214b is hydrogen/helium dominated then this allows us to place a constraint on the planet's bulk composition, namely its core, mantle and possibly its ice layer (Rogers & Seager 2010; Nettelmann et al. 2011). This is because the lighter atmospheric composition of a hydrogen/helium atmosphere, compared to for instance a water-world composition, requires a heavier interior composition of silicates, ferrous material or ices to compensate in order to fit the observed mass and radius—and thus density—constraints of Charbonneau et al. (2009). We compare our results to two numerical models (Rogers & Seager 2010; Nettelmann et al. 2011) that attempt to determine the range of realistic bulk compositions that agree with the observed mass and radius constraints. Regardless of whether the planet's hydrogen/helium envelope is primordial or due to outgassing, it is expected that this atmospheric layer will be a small percentage (~5%) of this planet's total mass (Rogers & Seager 2010; Nettelmann et al. 2011). Nettelmann et al. (2011) and Rogers & Seager (2010) predict, under their hydrogen/helium atmosphere scenarios, that a wide range of core/mantle masses is still viable (from a few percent to ~99% of the mass of GJ 1214b). The higher core/mantle masses result from a planet with very little water, while for the lower masses it would entail a massive interior water/ice layer. Nettelmann et al. (2011) suggest that if this planet's atmosphere is dominated by hydrogen and helium then one can place an upper limit on the water-to-rock ratio of approximately six-to-one; the true value of this quantity is expected to be much lower, and thus the core mass is expected to makeup at least ~14% of the planet's mass and likely much more (Nettelmann et al. 2011).

5. CONCLUSIONS

We report observations of four transits of GJ 1214b using WIRCam on the CFHT. We observed nearly simultaneously in the J band and in the K_s band for three of the transits, and in the J band and the CH_4On filter in another. Our best-fit J-band transit depth is consistent with the values obtained in the optical and very near-infrared: $(R_{PJ}/R_*)^2 = 1.338 \pm 0.013\%$. Our K_s-band transit is deeper: $(R_{PKs}/R_*)^2 = 1.438 \pm 0.019\%$. Our J- and K_s-band transit depths are inconsistent at the 5σ level. The impact of spots and rotational modulation on the transit depths we observe should be small; nevertheless spots will induce small changes in the transit depths we measure from epoch to epoch, and as a result a better metric to quantify our observations may be the factor that the K_s-band transits are deeper than the J-band transits observed simultaneously. Our K_s-band transits display a deeper depth than our J-band transits by a factor of $(R_{PKs}/R_{PJ})^2 = 1.072 \pm 0.018$. We thus detect increased transit depths in our broadband K_s band (~2.15 μm) as compared to the J band (~1.25 μm) with 4σ confidence. The difference in transit depth between the two bands that we measure is best explained as due to a spectral absorption feature from the atmosphere of GJ 1214b; the only way to get a spectral absorption feature this prominent is if the atmosphere of GJ 1214b has a large-scale

height, low mean molecular weight and is thus hydrogen/helium dominated. Water or methane are possible opacity sources to explain this absorption. If GJ 1214b's atmosphere is hydrogen/helium dominated a range of core/mantle masses and ice layers is still viable, but the planet must have a large rocky core/mantle interior to its gaseous envelope. In this case, our increased K_s-band transit depth would be the first detection of a spectral feature in a super-Earth atmosphere, and GJ 1214b would best be described as a mini-Neptune.

However, when combining our observations with other observations of GJ 1214b, most specifically the lack of spectral features observed in the Bean et al. (2010) VLT/FORS2 spectrophotometry from 0.78 to 1.0 μm, the atmospheric composition of GJ 1214b is less clear. There are several leading possibilities. One possibility remains that the atmosphere of GJ 1214b is water-vapor dominated and our increased K_s-band transit depth is simply an outlier; our increased K_s-band transit depth will have to be reconfirmed or spectral features at other wavelengths will have to be detected before this scenario can be confidently ruled out. The possibility that is arguably the most consistent with all the observed data to date, is that GJ 1214b has a hydrogen/helium-dominated atmosphere with a haze layer at high altitude consisting of particles that can be no smaller than approximately sub-micron in size; such a scenario would explain the lack of observed spectral absorption features in the very near-infrared in the Bean et al. (2010) spectrophotometry and our own increased K_s-band transit depth if there is an opacity source at $\sim$2.15 μm. Lastly, we note that the true spectrum of GJ 1214b could be more complicated than our models predict for a variety of reasons—one such possibility is the importance of non-equilibrium chemistry in GJ 1214b's atmosphere which would alter GJ 1214b's predicted transmission spectrum (Miller-Ricci Kempton et al. 2011).

Clearly, further observations are required to precisely determine the nature of GJ 1214b's atmosphere. We encourage further observations to confirm our increased K_s-band transit depth. We plan to use the CFHT/WIRCam to reobserve the transit of GJ 1214b in K_s band on several occasions in the Spring/Summer 2011 observing season.

The Natural Sciences and Engineering Research Council of Canada supports the research of B.C. and R.J. E.M-R.K.'s work was performed under contract with the California Institute of Technology funded by NASA through the Sagan Fellowship Program. The authors thank the anonymous referee and the great many other people who commented on and improved this manuscript prior to publication. The authors especially appreciate the hard work and diligence of the CFHT staff for both scheduling these challenging observations and ensuring that these "Staring Mode" observations were successful.

REFERENCES

Andrae, R., et al. 2010, arXiv:1012.3754
Brown, T. M., et al. 2001, ApJ, 553, 1006
Bean, J. L., Kempton, E. M.-R., & Homeier, D. 2010, Nature, 468, 669
Berta, Z., et al. 2010, arXiv:1012.0518
Carter, J. A., et al. 2011, ApJ, 730, 82
Charbonneau, D., et al. 2009, Nature, 462, 891
Claret, A. 1998, A&A, 335, 647
Croll, B. 2006, PASP, 118, 1351
Croll, B., et al. 2010a, ApJ, 717, 1084
Croll, B., et al. 2010b, ApJ, 718, 920
Croll, B., et al. 2011, AJ, 141, 30
Czesla, S., et al. 2009, A&A, 505, 1277
Desert, J.-M., et al. 2011, ApJ, 731, 40
Devost, D., et al. 2010, Proc. SPIE, 77372D
Dittman, J. A., et al. 2009, ApJ, 701, 756
Eastman, J., et al. 2010, PASP, 122, 935
Fortney, J. J. 2005, MNRAS, 364, 649
Griffith, C. A. 1993, Nature, 364, 511
Hansen, J. E., & Travis, L. D. 1974, Space Sci. Rev., 16, 527
Hauschildt, P. H., et al. 1997a, ApJ, 483, 390
Hauschildt, P. H., et al. 1997b, ApJ, 488, 428
Irwin, J., et al. 2009, ApJ, 701, 1436
Lecavelier des Etangs, A., et al. 2008, A&A, 481, L83
Leger, A., et al. 2009, A&A, 506, 287
Lester, J. B., & Neilson, H. R. 2008, A&A, 491, 633
Liddle, A. R. 2007, MNRAS, 377, L74
Mandel, K., & Agol, E. 2002, ApJ, 580, L171
Mayor, M., et al. 2009a, A&A, 493, 639
Mayor, M., et al. 2009b, A&A, 507, 487
Miller-Ricci, E., & Fortney, J. J. 2010, ApJ, 716, L74
Miller-Ricci Kempton, E., Zahnle, K., & Fortney, J. J. 2011, ApJ, submitted (arXiv:1104.5477)
Moses, J. I., et al. 2005, J. Geophys. Res., 110, E8
Nettelmann, N., et al. 2011, ApJ, 733, 2
Nutzman, P., & Charbonneau, D. 2008, PASP, 120, 317
Pont, F., et al. 2007, A&A, 476, 1347
Pont, F., et al. 2008, MNRAS, 385, 109
Pont, F., et al. 2011, MNRAS, 411, 1953
Queloz, D., et al. 2009, A&A, 506, 303
Rabus, M., et al. 2009, A&A, 494, 391
Rages, K., et al. 1999, Icarus, 139, 211
Rogers, L. A., & Seager, S. 2010, ApJ, 716, 1208
Sada, P. V., et al. 2010, ApJ, 720, L215
Sing, D. K., et al. 2011, MNRAS, submitted (arXiv:1103.0026)
Tomasko, M. G., et al. 2008, Icarus, 56, 669
Udry, S. 2007, A&A, 469, L43
Winn, J. N., et al. 2009, ApJ, 693, 794
Zahnle, K. 2009, ApJ, 701, L20
Zboril, M. 2003, Astron. Nachr., 324, 527